Computer simulations of electrorheological fluids in the dipole-induced dipole model

Y. L. Siu, Jones T. K. Wan, and K. W. Yu
Department of Physics, The Chinese University of Hong Kong, Shatin, New Territories, Hong Kong, China
(Received 12 June 2001; published 23 October 2001)

We have employed the multiple image method to compute the interparticle force for a polydisperse electrorheological (ER) fluid in which the suspended particles can have various sizes and different permittivities. The point-dipole (PD) approximation, being routinely adopted in the computer simulation of ER fluids, is known to err considerably when the particles approach and finally touch due to multipolar interactions. The PD approximation becomes even worse when the dielectric contrast between the particles and the host medium is large. From the results, we show that the dipole-induced-dipole (DID) model yields very good agreements with the multiple image results for a wide range of dielectric contrasts and polydispersity. As an illustration, we have employed the DID model to simulate the athermal aggregation of particles in ER fluids, both in uniaxial and rotating fields. We find that the aggregation time is significantly reduced. The DID model partially accounts for the multipolar interaction and is simple to use in the computer simulation of ER fluids.

DOI: 10.1103/PhysRevE.64.051506 PACS number(s): 83.80.Gv, 82.70.Dd, 41.20.−q

I. INTRODUCTION

The prediction of the yield stress for electrorheological (ER) fluids is the main concern in theoretical investigations of ER fluids. Early studies failed to derive the experimental yield stress data [1] because these studies were almost based on a point-dipole approximation [2,3]. The point-dipole approximation is routinely adopted in computer simulations because it is simple and easy to use. Since many-body and multipolar interactions between particles have been neglected, the strength of ER effects predicted by this model is of an order lower than the experimental results. Hence, substantial effort has been made to sort out more accurate models.

Klingenberg and co-workers developed an empirical force expression from a numerical solution of Laplace's equation [4]. Davis used the finite-element method [5]. Clercx and Bossis developed a full multipolar treatment to account for the multipolar polarizability of spheres up to 1000 multipolar orders [6]. Yu and co-workers developed an integral equation method that avoids the match of complicated boundary conditions on each interface of the particles and is applicable to nonspherical particles and multimedia [7]. Although the above methods are accurate, they are relatively complicated to use in the dynamic simulation of ER fluids. Alternative models have been developed to circumvent the problem: the coupled-dipole model [8] and the dipole-induced-dipole (DID) model [9], which take care of mutual polarization effects when the particles approach and finally touch.

The DID model accounts for multipolar interactions partially and is simple to use in computer simulation of ER fluids [9]. As an illustration, we employed the DID model to simulate the athermal aggregation of particles in ER fluids both in uniaxial and rotating fields. We find that the aggregation time is significantly reduced. In Sec. II, we review the multiple image method and establish the DID model. In Sec. III, we apply the DID model to the computer simulation of ER fluids in a uniaxial field. In Sec. IV, we extend the simulation to athermal aggregation in rotating fields. Discussion of our results will be given in Sec. V.

II. IMPROVED MULTIPLE IMAGE METHOD

Here we briefly review the multiple images method [9] and extend the method slightly to handle different dielectric constants. Consider a pair of dielectric spheres, of radii a and b, dielectric constants ϵ_1 and ϵ_1', respectively, separated by a distance r. The spheres are embedded in a host medium of a dielectric constant ϵ_2. Upon the application of an electric field $\mathbf{E}_0$, the induced-dipole moment inside the spheres are, respectively, given by (SI units)

$$p_{a0}=4\pi\epsilon_0\epsilon_2\beta E_0 a^3, \quad p_{b0}=4\pi\epsilon_0\epsilon_2\beta' E_0 b^3, \tag{1}$$

where the dipolar factors β,β' are given by

$$\beta=\frac{\epsilon_1-\epsilon_2}{\epsilon_1+2\epsilon_2}, \quad \beta'=\frac{\epsilon_1'-\epsilon_2}{\epsilon_1'+2\epsilon_2}. \tag{2}$$

From the multiple image method [9], the total dipole moment inside sphere a is

$$p_{aT}=(\sinh\alpha)^3\sum_{n=1}^{\infty}\left[\frac{p_{a0}b^3(-\beta)^{n-1}(-\beta')^{n-1}}{(b\sinh n\alpha+a\sinh(n-1)\alpha)^3}+\frac{p_{b0}a^3(-\beta)^n(-\beta')^{n-1}}{(r\sinh n\alpha)^3}\right], \tag{3}$$

$$p_{aL}=(\sinh\alpha)^3\sum_{n=1}^{\infty}\left[\frac{p_{a0}b^3(2\beta)^{n-1}(2\beta')^{n-1}}{(b\sinh n\alpha+a\sinh(n-1)\alpha)^3}+\frac{p_{b0}a^3(2\beta)^n(2\beta')^{n-1}}{(r\sinh n\alpha)^3}\right], \tag{4}$$

where the subscripts $T(L)$ denote a transverse (longitudinal) field, i.e., the applied field is perpendicular (parallel) to the line joining the centers of the spheres. Similar expressions for the total dipole moment inside sphere b can be obtained by interchanging a and b, as well as β and β'. The parameter α satisfies

$$\cosh\alpha=\frac{r^2-a^2-b^2}{2ab}.$$

In Ref. [9], we checked the validity of these expressions by comparing with the integral equation method. We showed that these expression are valid at high contrast. Our improved expressions will be shown to be good at low contrast as well (see below).

The force between the spheres is given by [10]

$$F_T=\frac{E_0}{2}\frac{\partial}{\partial r}(p_{aT}+p_{bT}),\quad F_L=\frac{E_0}{2}\frac{\partial}{\partial r}(p_{aL}+p_{bL}). \quad (5)$$

For monodisperse ER fluids ($a=b$, $\beta=\beta'$ and $p_a=p_b=p_0$), Klingenberg defined an empirical force expression [4]:

$$\frac{\mathbf{F}}{F_{PD}}=(2K_\parallel\cos^2\theta-K_\perp\sin^2\theta)\hat{\mathbf{r}}+K_\Gamma\sin 2\theta\hat{\theta}, \quad (6)$$

being normalized to the point-dipole (PD) force $F_{PD}=-3p_0^2/r^4$, where $K_\parallel$, $K_\perp$, and K_Γ (all tending to unity at large separations) are three force functions being determined from the numerical solution of Laplace's equation. The Klingenberg's force functions can be shown to relate to our multiple image moments as follows (here $a=b$, $\beta=\beta'$, and $p_a=p_b$):

$$K_\parallel=\frac{1}{2}\frac{\partial\tilde{p}_L}{\partial r},\quad K_\perp=-\frac{\partial\tilde{p}_T}{\partial r},\quad K_\Gamma=\frac{1}{r}(\tilde{p}_T-\tilde{p}_L), \quad (7)$$

where $\tilde{p}_L=p_L/F_{PD}E_0$ and $\tilde{p}_T=p_T/F_{PD}E_0$ are the reduced multiple image moments of each sphere. We computed the numerical values of these force functions separately by the approximant of Table I of the second reference of Ref. [4] and by Eq. (7).

In Fig. 1, we plot the multiple image results and the Klingenberg's empirical expressions. We show results for the perfectly conducting limit ($\beta=1$) only. For convenience, we define the reduced separation $\sigma=r/(a+b)$. For reduced separation $\sigma>1.1$, simple analytic expressions were adopted by Klingenberg. As evident from Fig. 1, the agreement with the multiple image results is impressive at large reduced separation $\sigma>1.5$, for all three empirical force functions. However, significant deviations occur for $\sigma<1.5$, especially for $K_\parallel$. For $\sigma\leqslant 1.1$, alternative empirical expressions were adopted by Klingenberg. For $K_\perp$, the agreement is impressive, although there are deviations for the other two functions. From the comparison, we would say that reasonable agreements have been obtained. Thus, we are confident that the multiple image expressions give reliable results.

The analytic multiple image results can be used to compare among the various models according to how many terms are retained in the multiple image expressions: (a) PD model: $n=1$ term only, (b) DID model: $n=1$ to $n=2$ terms only, and (c) multipole-induced-dipole (MID) model: $n=1$ to $n=\infty$ terms.

In a previous work [9], we examined the case of different size but equal dielectric constant ($\beta=\beta'$) only. Here we

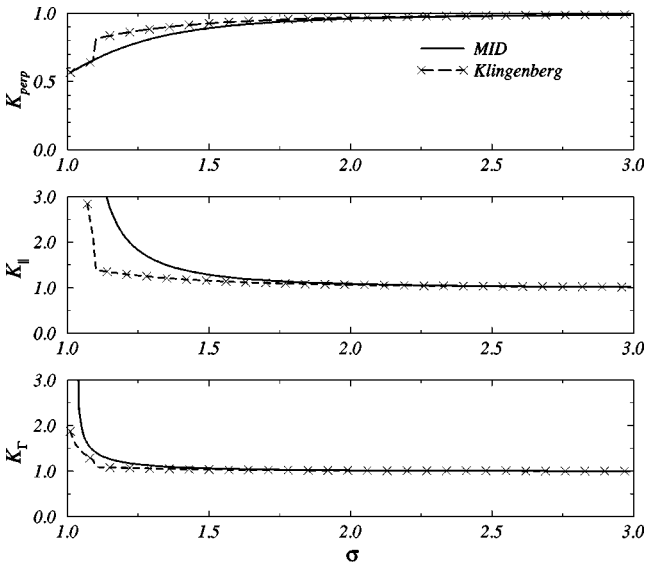

FIG. 1. The comparison of the multiple image results with Klingenberg's three force functions. $K_\perp$, $K_\parallel$, and K_Γ are plotted as functions of the reduced separation between two spherical particles.

focus on the case $a=b$ and study the effect of different dielectric constants. In Fig. 2, we plot the interparticle force in the longitudinal field case against the reduced separation σ between the spheres for (a) $\beta=9/11$ ($\epsilon_1/\epsilon_2=10$) and (b) $\beta=1/3$ ($\epsilon_1/\epsilon_2=2$) and various β'/β ratios. At low contrast, the DID model almost coincides with the MID results. In contrast, the PD model exhibits significant deviations. It is evident that the DID model generally gives better results than PD for all polydispersity.

III. COMPUTER SIMULATION IN THE DID MODEL

The multiple image expressions [Eqs. (3) and (4)] allows us to calculate the correction factor defined as the ratio between the DID and PD forces:

$$\frac{F_{DID}^{(\perp)}}{F_{PD}^{(\perp)}}=1-\frac{\beta a^3r^5}{(r^2-b^2)^4}-\frac{\beta' b^3r^5}{(r^2-a^2)^4}+\frac{\beta\beta' a^3b^3(3r^2-a^2-b^2)}{(r^2-a^2-b^2)^4}, \quad (8)$$

$$\frac{F_{DID}^{(\parallel)}}{F_{PD}^{(\parallel)}}=1+\frac{2\beta a^3r^5}{(r^2-b^2)^4}+\frac{2\beta' b^3r^5}{(r^2-a^2)^4}+\frac{4\beta\beta' a^3b^3(3r^2-a^2-b^2)}{(r^2-a^2-b^2)^4}, \quad (9)$$

$$\frac{F_{DID}^{(\Gamma)}}{F_{PD}^{(\Gamma)}}=1+\frac{\beta a^3r^3}{2(r^2-b^2)^3}+\frac{\beta' b^3r^3}{2(r^2-a^2)^3}+\frac{3\beta\beta' a^3b^3}{(r^2-a^2-b^2)^3}, \quad (10)$$

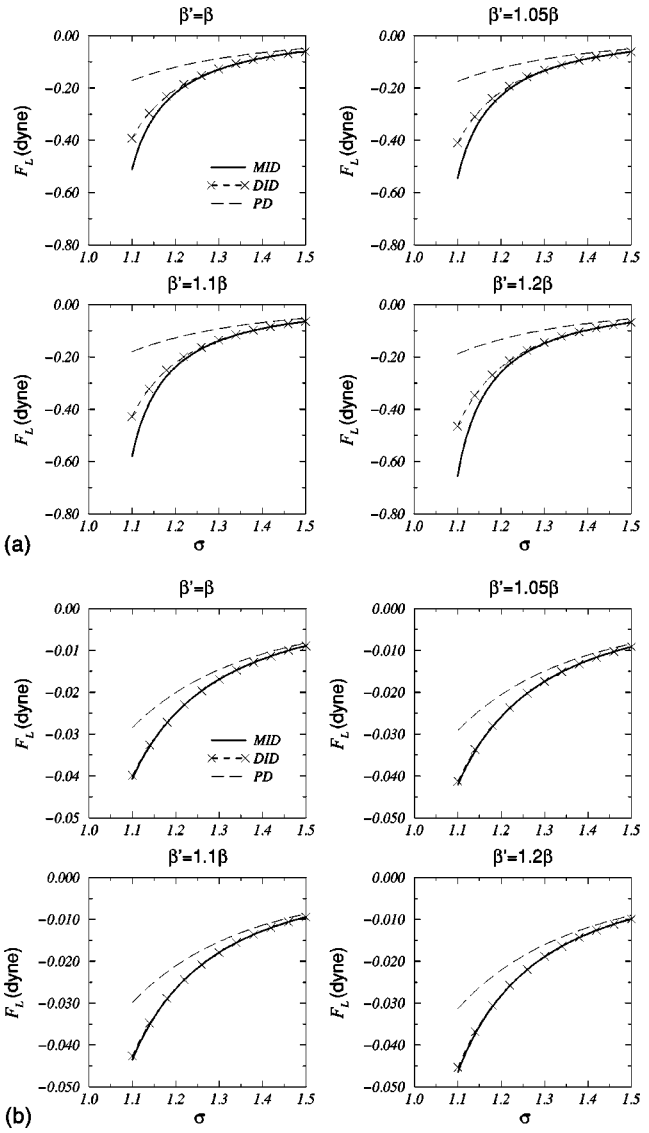

FIG. 2. The interparticle force plotted against the reduced separation σ between two spherical particles for several dipole factors β' of one spherical particle in units of β for longitudinal fields: (a) $\beta=9/11$ and (b) $\beta=1/3$.

where $F_{PD}^{(\perp)}=3p_{a0}p_{b0}/r^4$, $F_{PD}^{(\parallel)}=-6p_{a0}p_{b0}/r^4$, and $F_{PD}^{(\Gamma)}=-3p_{a0}p_{b0}/r^4$ are the point-dipole forces for the transverse, longitudinal, and Γ cases, respectively. These correction factors can be readily calculated in the computer simulation of polydisperse ER fluids. The results show that the DID force deviates significantly from the PD force at high contrast when β and β' approach unity. The dipole induced interaction will generally decrease (increase) the magnitude of the transverse (longitudinal) interparticle force with respect to the PD limit.

For simplicity, we consider the case of two equal spheres of radius a, initially at rest and at a separation d_0. An electric field is applied along the line joining the centers of the sphere. The equation of motion is given by

$$\frac{dz}{dt}=F_{\parallel}(2z), \tag{11}$$

where z is the displacement of one sphere from the center of mass. The separation between the two spheres is thus $d=2z$ and the initial condition is $d=d_0$ at $t=0$. Equation (11) is a dimensionless equation. We have chosen the following natural scales to define the dimensionless variables:

$$\text{length } \sim a, \quad \text{time } = t_0 \sim \frac{6\pi\eta_c a^2}{F_0},$$

$$\text{force } = F_0 \sim \frac{\epsilon_0 \epsilon_2^2 a^2 E_0^2}{4\pi},$$

where E_0 is the field strength, m is the mass, and η_c is the coefficient of viscosity. Using typical parameters, we find t_0 is of the order of milliseconds. We have followed Klingenberg [2,3] to ignore the inertial effect, captured by the parameter G:

$$G=\frac{\epsilon_0 m \epsilon_2^2 E_0^2}{144\pi^3 \eta_c^2 a}.$$

The neglect of G can be justified as follows. For values common to the ER suspension: $\eta_c \approx 0.1$ Pa s, $m \approx 8\times10^{-13}$ kg, $a \approx 5\times10^{-6}$ m [2]. The inertial term G is of the order 10^{-8}. We also neglect the thermal motion of the particles, which is a valid assumption at high fields. We should remark that the initial separation d_0 is related to the volume fraction ϕ, defined as the ratio of the volume of the sphere to that of the cube, which contains the sphere [3], i.e., $\phi=V_{\text{sphere}}/V_{\text{cube}}$, and

$$\frac{d_0}{2a}=\left(\frac{\pi}{6\phi}\right)^{1/3}.$$

For the PD approximation, Eq. (11) admits an analytic solution:

$$z=\left[\left(\frac{d_0}{2}\right)^5-\frac{15p_0^2 t}{8}\right]^{1/5}. \tag{12}$$

We integrate the equation of motion by the fourth-order Runge-Kutta algorithm, with time steps $\delta t=0.01$ and 0.001 for small and large volume fractions, respectively. We plot the displacement d/a vs the time graph (not shown here) for the PD case and find excellent agreement between analytic and numerical results.

For the DID model, we have to integrate the equation of motion numerically. In Fig. 3, we plot the displacement d/a vs the time graph for the aggregation of two spheres in uniaxial fields. At small volume fractions, i.e., when the initial separation is large, the time for aggregation is large and the DID results deviate slightly from the PD results. However, at large volume fractions, the DID results are significantly smaller than the PD calculations. The effect becomes even more pronounced at large β.

In Fig. 4(a), we plot the ratio of aggregation time of the DID to PD cases. The results showed clearly that the aggregation time has been significantly reduced when mutual po-

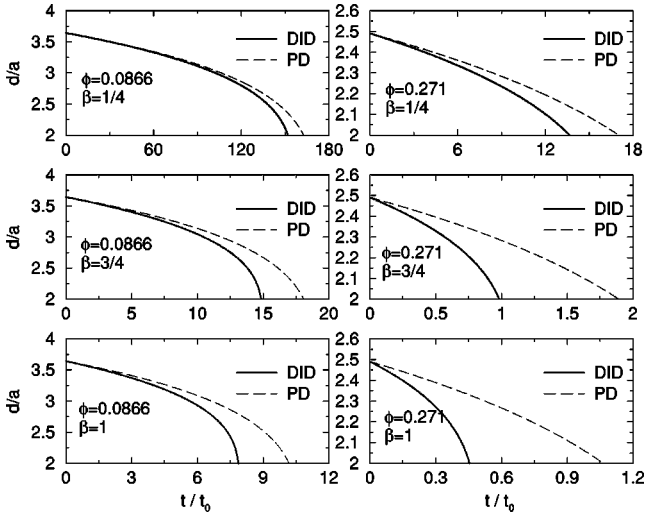

FIG. 3. The displacement-time graph for athermal aggregation of two spherical particles in a uniaxial field for various volume fractions and dipole factors.

larization effects are considered. The reduction in aggregation time becomes even more pronounced for small initial separations.

IV. ATHERMAL AGGREGATION IN THE ROTATING FIELD

Recently, Martin and co-workers [11] demonstrated athermal aggregation with the rotating field. When a rotating field is applied in the x-y plane at a sufficiently high frequency that particles do not move much in one period, an average attractive dipolar interaction is created. The result of this is the formation of plates in the x-y plane. Consider a rotating field applied in the x-y plane: $E_x = E_0 \cos \omega t, E_y = E_0 \sin \omega t$. The dimensionless equation of motion for the two sphere case becomes

$$\frac{dx}{dt} = F_{\parallel} \cos^2 \omega t + F_{\perp} \sin^2 \omega t, \quad \frac{dy}{dt} = -F_{\Gamma} \sin 2\omega t, \tag{13}$$

where (x,y) is the displacement of one sphere from the center of mass. For large ω, we may safely neglect the y component of the motion. In the PD approximation, $F_{\parallel} = -6p_0^2/r^4$ and $F_{\perp} = 3p_0^2/r^4$, we find the analytic result

$$x = \left[\left(\frac{d_0}{2} \right)^5 - \frac{15 p_0^2}{64\omega} (2\omega t + 3 \sin 2\omega t) \right]^{1/5}. \tag{14}$$

The separation between the two spheres is just $d = 2x$, with the initial separation $d = d_0$ at $t = 0$. In the rotating field case, we also integrate the equation of motion by the fourth-order Runge-Kutta algorithm, but with $\delta t = 1/(4\omega)$ and $1/(40\omega)$ as the time steps. Note that $\delta t = 1/(4\omega)$ should be the largest time step that can be used because we must at least go through a cycle consisting of the transverse and longitudinal

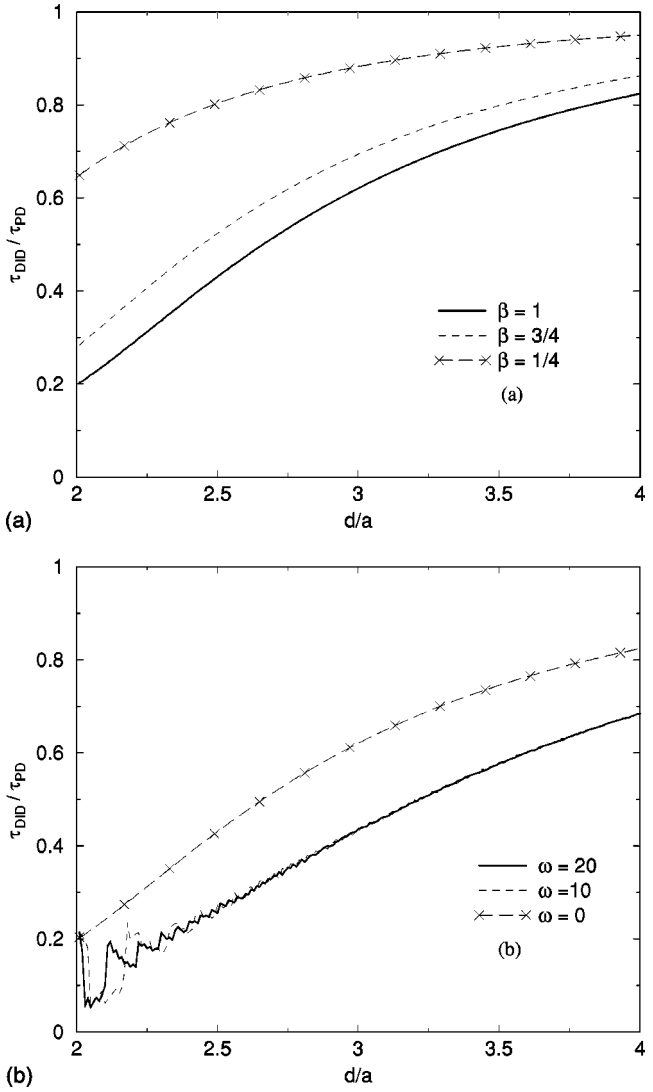

FIG. 4. The reduction factor of the aggregation time of two spherical particles plotted against the initial separation for (a) uniaxial field and (b) rotating field. τ_{DID} and τ_{PD} are the aggregation times in the DID and PD models, respectively.

field cases. The oscillating effect of a rotating field is less observable when the time step is smaller than this maximum value.

We plot the displacement vs time graph (not shown here) for the PD case in a rotating field and find an excellent agreement between analytic and numerical results. It is found that the aggregation time is four times of that of the uniaxial field case. In fact, Eq. (14) reduces to Eq. (12) as $\omega \to 0$. However, at large ω, Eq. (14) becomes

$$x = \left[\left(\frac{d_0}{2} \right)^5 - \frac{15 p_0^2 t}{32} \right]^{1/5}.$$

That is, in the PD approximation, the time-average force becomes 1/4 of that of the uniaxial field case. It is because the two dipole moments spend equal times in the transverse and longitudinal orientations, while $F_{\parallel} = -2F_{\perp}$ in the PD case, leading to an overall attractive force that is 1/4 of the

force of the uniaxial field case. When the multiple image force is included, we expect that the magnitude of $F_{\parallel}$ increases while that of $F_{\perp}$ decreases and we expect an even larger attractive force when the spheres approach. In this case, the aggregation time must be reduced even more significantly.

In Fig. 4(b), we plot the ratio of the aggregation time of the DID to PD cases for $\beta=1$ and several ω. The $\omega=0$ curve is just for the uniaxial field case. The results showed clearly that the aggregation time has been significantly reduced when mutual polarization effects are considered. The reduction in aggregation time becomes even pronounced for small initial separations. It is observed that fluctuations exist when the initial separation between the spheres is $2.4a$ or less. It is because the motion is sensitive to the initial orientation of the dipoles when the spheres are too close.

Similarly, we consider the aggregations of three and four equal spheres, arranged in a chain, an equilateral triangle and a square. For a chain of three spheres in a rotating field, the central sphere does not move, while the two spheres at both ends move towards the central sphere. For three spheres in an equilateral triangle, the center of mass (c.m.) will not move while each sphere moves towards the c.m., subject to the force of the other two spheres. The same situation occurs for four spheres in a square, in which each sphere moves towards the c.m., subject to the force of the other three spheres.

In the PD approximation, we report the analytic results as follows. For three spheres in a chain,

$$x=\left[d_0^5-\frac{255p_0^2}{64\omega}(2\omega t+3\sin 2\omega t)\right]^{1/5}. \tag{15}$$

For three spheres in an equilateral triangle,

$$x=\left[\left(\frac{d_0}{\sqrt{3}}\right)^5-\frac{5p_0^2}{8\sqrt{3}\omega}(4\omega t-\sin 2\omega t)\right]^{1/5}. \tag{16}$$

For four spheres in a square,

$$x=\left[\left(\frac{d_0}{\sqrt{2}}\right)^5-\frac{15p_0^2}{8\omega}\left(\frac{4\sqrt{2}+1}{4}\omega t-\frac{8\sqrt{2}-3}{8}\sin 2\omega t\right)\right]^{1/5}. \tag{17}$$

In each of the above cases, x is the distance of one sphere from the center of mass. In the case of three spheres in a chain, the separation between the spheres is the same as $d=x$. In the case of three spheres in an equilateral triangle, the separation between spheres is $d=\sqrt{3}x$. In the case of four spheres in a square, the separation between spheres is $d=\sqrt{2}x$. Again, we integrate the equation of motion by the fourth-order Runge-Kutta algorithm. We find excellent agreements between the analytic and numerical results (not shown here).

It has been found that the displacement in the y direction is about 0.5% for $\omega=5$ and a larger ω has been used in the simulation. On the other hand, it is time consuming for simulations with $\omega>20$. It is evident from the displacement-time graph that the results are correct. In Fig. 5, the oscillation amplitude is reduced when the rotating frequency increases in the simulation. This is consistent with the assumption made in our analytic expressions. In Fig. 6, it is observed that fluctuations exist when the initial separation between the spheres is $2.4a$ or less in all three graphs. Again, it is because the motion is sensitive to the orientation of the dipoles when the spheres are close. From the simulation, the reduction effects become even more pronounced for the rotating electric field case than the uniaxial field case.

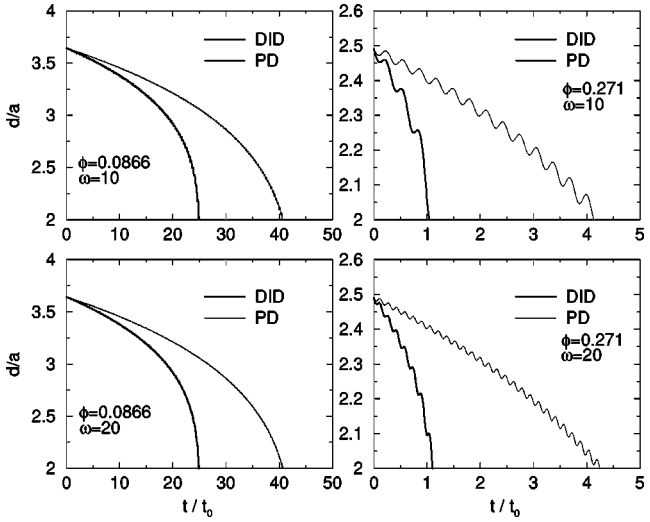

FIG. 5. The displacement-time graph for the athermal aggregation of two spherical particles in a rotating field for various volume fractions and dipole factors.

V. DISCUSSION AND CONCLUSION

Here a few comments on our results are in order. Bonnecaze and Brady [14] included corrections to PD by means of

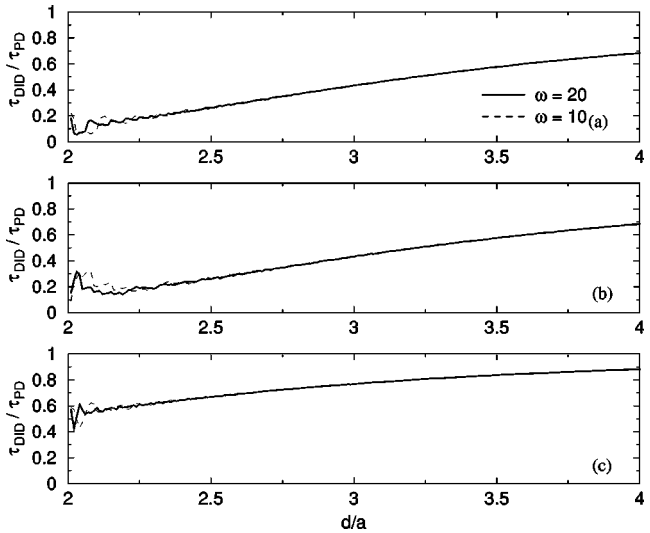

FIG. 6. The reduction of the aggregation time for clusters of three and four spherical particles plotted against the initial separation in the rotating field. τ_{DID} and τ_{PD} are the aggregation times in the DID and PD models, respectively.

an energy approach. In their approach, both the long-range many-body interactions and the lubricationlike near-field interactions are included in the computer simulations. The comparison to our approach will be a topic for future work. We believe that the multipolar interactions are more important than the many-body (local-field) effects. In Ref. [8], as well as Ref. [15], the particles in ER fluids are treated as point dipoles while their dipole moments are determined by adding the local-field corrections. In our model, the particles are treated as extended dielectric spheres. The additional terms in DID arise from multipole interactions, rather than from local-field corrections. In this regard, the DID model is adequate for aggregation problems while it may be unsatisfactory for calculating shear stresses in ER fluids due to large multipole interactions for touching spheres. For shear stresses, however, we had better use the more accurate MID model.

In this work, we studied the aggregation time for several particles. We should also examine the morphology of aggregation, due to multiple image forces. In this connection, we can also examine the structural transformation by applying the uniaxial and rotating fields simultaneously [12].

We have done simulation in the monodisperse case. Real ER fluids must be polydisperse in nature: the suspending particles can have various sizes or different permittivities. Polydisperse ER fluids have attracted considerable interest recently because the size distribution and dielectric properties of the suspending particles can have significant impact on the ER response [13]. We should extend the simulation to the polydisperse case by using the DID model.

In summary, we have used the multiple image to compute the interparticle force for a polydisperse electrorheological fluid. We apply the formalism to a pair of spheres of different dielectric constants and calculate the force as a function of the separation. The results show that the PD approximation is oversimplified. It errs considerably because many-body and multipolar interactions are ignored. The DID model accounts for multipolar interactions partially and yields overall satisfactory results in the computer simulation of ER fluids while it is easy to use.

ACKNOWLEDGMENTS

This work was supported by the Research Grants Council of the Hong Kong SAR Government under Grant No. CUHK4284/00P. We thank Dr. Z. W. Wang for sending us a program on computer simulation of electrorheological fluids. Y.L.S. is grateful to M. L. Wong for her helpful advice in programming throughout the course of this work. K.W.Y. acknowledges useful discussions with Professor G. Q. Gu.

[1] P. M. Adriani and A. P. Gast, Phys. Fluids **31**, 2757 (1988).
[2] D. J. Klingenberg, F. van Swol, and C. F. Zukoski, J. Chem. Phys. **91**, 7888 (1989).
[3] D. J. Klingenberg, F. van Swol, and C. F. Zukoski, J. Chem. Phys. **94**, 6160 (1991).
[4] D. J. Klingenberg and C. F. Zukoski, Langmuir **6**, 15 (1990); D. J. Klingenberg, F. van Swol, and C. F. Zukoski, J. Chem. Phys. **94**, 6170 (1991).
[5] L. C. Davis, Appl. Phys. Lett. **60**, 319 (1992).
[6] H. J. H. Clercx and G. Bossis, Phys. Rev. E **48**, 2721 (1993).
[7] K. W. Yu, Hong Sun, and Jones T. K. Wan, Physica B **279**, 78 (2000).
[8] Z. W. Wang, Z. F. Lin, and R. B. Tao, Int. J. Mod. Phys. B **10**, 1153 (1996).
[9] K. W. Yu and Jones T. K. Wan, Comput. Phys. Commun. **129**, 177 (2000).
[10] J. D. Jackson, *Classical Electrodynamics* (Wiley, New York, 1975).
[11] J. E. Martin, R. A. Anderson, and C. P. Tigges, J. Chem. Phys. **108**, 3765 (1998); **108**, 7887 (1998).
[12] C. K. Lo and K. W. Yu, Phys. Rev. E (to be published).
[13] M. Ota and T. Miyamoto, J. Appl. Phys. **76**, 5528 (1994).
[14] R. T. Bonnecaze and J. F. Brady, J. Chem. Phys. **96**, 2183 (1992); J. Rheol. **36**, 73 (1992).
[15] L. C. Davis, J. Appl. Phys. **72**, 1334 (1992).